RESEARCH ON THE USE OF DRONES IN PRECISION AGRICULTURE

George IPATE[1], Gheorghe VOICU[2], Ion DINU[3]

Technological progress made in monitoring, supervision, management and control systems have opened a new era in which many traditional agricultural practices are outdated. Their replacement with new technologies falls into the "precision farming" category, which translates into applying the agronomic variables in the right place, at the right time and with precise control over the amount of material inputs or crop production. Unmanned aircraft proved to be one of those techniques that allow rapid and nondestructive analysis of air quality, physical properties of the components of soil or crop growth. This research covers theoretical and experimental framework to develop an autonomous aerial vehicle capable of providing farmers very important information about the plant growth medium. Also aerial imagery inside or outside greenhouses can reveal areas where problems exist to better manage them.

Keywords: precision agriculture, quadcopter, greenhouse, image processing.

1. Introduction

Apart favorable climatic conditions for growing vegetables, our country still has no leading technical facilities, necessary for the competitiveness of the market economy. Thus, any solution by which farmers can reduce production costs while maintaining product quality and integrity is considered. Unmanned Aerial Vehicles (UAVs) are used by over five years in precision agriculture for a number of missions, including capturing image for analysis of individual plant leaves culture, obtaining information on soil water holding capacity or management irrigation systems especially for large agricultural producers that cultivate in regions with dispersed areas. In the design, development and implementation of UAV systems there are integrated many disciplines of engineering such as aerodynamics, electronics, materials structure, computer programming, economy, and as technology progresses very quickly the level of knowledge in the respective fields must be continuously adapted.

The quadcopter can be described as a UAV with four propellers in a cross configuration, which can be remotely controlled aircraft or can fly autonomously

---

[1] Lect., Dept.of Biotechnical Systems, University POLITEHNICA of Bucharest, Romania, e-mail: puiuipate@yahoo.com
[2] Prof., Dept.of Biotechnical Systems, University POLITEHNICA of Bucharest, Romania
[3] Prof., Dept.of Mechanics, University POLITEHNICA of Bucharest, Romania

based on pre-programmed flight plans or on more complex dynamic automation systems [1-7].

At present, UAVs are also being employed in various commercial and industrial applications. In particular, these include the use of unmanned helicopters for crop dusting or precision farming. Sugiura et al. (2003) used an imaging sensor and laser range finder mounted on an unmanned helicopter, to generate maps of field information such as crop status and land topographical feature [8]. Archer et al. (2004) develop a microwave autonomous copter system for monitoring the temporal changes of soil moisture as a function of depth, even in the presence of vegetative covers [9]. Khan et al. (2010) demonstrated that the UAV sensors can be used for satellite validation in the atmospheric boundary layer, for horizontal and vertical mapping of local pollutants and greenhouse gases, and for understanding carbon uptake in a forest canopy [10]. Patel et al. (2013) designed an innovative quadcopter to survey the agricultural farm by an infrared camera in order to show the difference between infected or diseased crop and matured crop [2]. Verbeke et al. (2014) tested a novel compound multicopter for inspecting fruit orchards and vineyards while flying in between the tree rows in outdoor conditions [4]. Several studies and research applications involving the modeling, design and control of multicopter have been performed by researchers and many solutions are proposed in the literature [1-6, 11-14]. We cite only two very interesting research. Achtelik et al. (2011) used a technology based on an infrared laser system who transforms the laser beam back to electrical energy to show unlimited flight time of a quadcopter [13]. Raza and Gueaieb (2010) describe the different steps of designing and testing a quadcopter. In their research, they proposed and implemented a fuzzy logic controller [14].

This paper presents a general guideline to design a mini quadrotor UAV. For identifying the quadrotor dynamical parameters an experimental method for determining thrust and drag coefficients was used. A simple algorithm is tested to an inertial measurement unit (IMU) to improve accuracy and sensor output for estimating the vehicle's orientation and altitude of the quadrotor and to be used as a basis for the controller design. The last part of the paper summarized the several applications of quadcopter in greenhouses surveillance. Farmers who have incorporated new technology into their operations take advantage of information about weather, crop modeling, soil moisture or environmental pollution.

2. Methodology

The main parts of a quadcopter: the frame connects all of the other components, it's shaped in either an X or a + shape and need to be strong, but also lightweight; rotors (coreless or brushless DC motors) that can provide the necessary thrust to propel the craft; an electronic speed controller to control

separately each rotor by specific needs; IMU sensors to measure the attitudes of the vehicles; microcontroller - "the brain" of quadcopter - an on-board processor that collects data, implement control algorithms, drive actuators and communicate with ground stations; propeller; battery is the power source for the whole quadcopter; radio control transmitter; optional-GPS, sensors, camera vision subsystem [2,5,6,8-12]. Schematic structure of the quadcopter is shown in fig. 1.
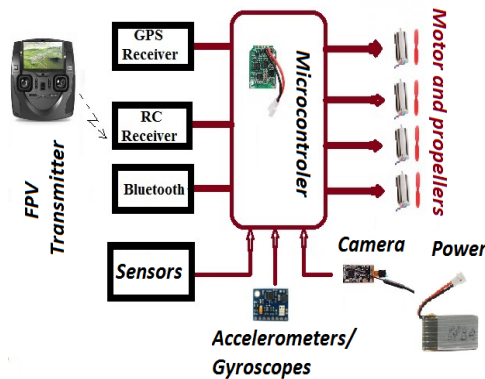

Fig. 1. Diagram of the electronic structure of quadcopter

Fig. 2. Conceptual model of a quadrotor dynamics

Dynamic modelling. A mathematical model of a quadrocopter consists of describing rigid body kinematics, dynamics of fixed and body reference frames and forces applied to the quadrocopter, and it can be done by Euler equations, Euler-Newton approach or Lagrangian approach [1,11]. The positions of the body-fixed axis of a rotating body is approximated through the use of Euler angles: spin φ, nutation θ and precession ψ. The angular velocities and angular accelerations which appear in Euler's equations are expressed in terms of these fundamental values, the positions of the principal axes being expressed as angular deviations from some initial positions [15,17]. The relationship between absolute angles φ (roll), θ (pitch), and ψ (yaw), and the angular rates is also complicated due to the fact that these quantities are defined in different coordinate frames as shown above in Fig. 2 [15,16].

From Fig. 2, the angular velocity of rotor i, denoted with ω_i, creates a thrust force T_i and drag moment τ_i. Based on the momentum theory, both thrust force and drag moment are proportional to the square of the angular speed of the propeller as stated in the following equations [16,18]:

$$T_i = K_T \omega_i^2 , \tag{1}$$
$$\tau_i = K_\tau \omega_i^2 ; \tag{2}$$

where, K_T and K_τ is the thrust force and drag moment coefficients, respectively.

Summing over all the motors, we find that the total thrust on the quadcopter (in the body frame) is given by [12,14,16]:

$$T = \sum_{i=1}^{4} T_i = k \begin{bmatrix} 0 \\ 0 \\ \sum \omega_i^2 \end{bmatrix}. \tag{3}$$

In the inertial frame, the acceleration of the quadcopter is due to thrust, gravity, and linear friction. The thrust vector can be obtain in the inertial frame by using the rotation matrix R to map the thrust vector from the body frame to the inertial frame. Thus, the linear motion can be summarized as [16]:

$$m\ddot{x} = \begin{bmatrix} 0 \\ 0 \\ -mg \end{bmatrix} + R \cdot T + F_D \tag{4}$$

where x is the position of the quadcopter, g is the acceleration due to gravity, F_D is the drag force, and T is the thrust vector in the body frame. In this equation R is the direction cosine transformation matrix, [18]:

$$R = \begin{bmatrix} c(\theta)c(\psi) & s(\theta)s(\psi) & -s(\theta) \\ c(\psi)s(\theta)s(\varphi) - s(\psi)c(\varphi) & s(\psi)s(\theta)s(\varphi) + c(\psi)c(\varphi) & c(\psi)c(\varphi) \\ c(\psi)s(\theta)s(\varphi) + s(\psi)s(\varphi) & s(\psi)s(\theta)c(\varphi) & c(\psi)c(\varphi) \end{bmatrix} \tag{5}$$

where c and s are cosine and sine, respectively.

Sensors. Inertial Measurement Unit (IMU) is an essential sensor to an unmanned aerial vehicles. It is attached to the aircraft to provide fundamental real-time motion data such as accelerations, angular rates, and magnetic values [17]. In the field of sensing technologies, manufacturers currently provide a new generation of integrated micro IMU composed generally of Micro Electro-Mechanical Systems (MEMS) technology inertial, magneto-resistive and barometric sensors. The typical accelerometer is composed of movable proof mass with plates that is suspended by compliant beams anchored to a fixed frame. External acceleration changes the capacitance between the plate and the surrounding walls. The output of the accelerometers is given by [15]:

$$y_{acc} = k_{acc}A + \beta_{acc} + \eta_{acc}, \tag{6}$$

where y_{acc} is in Volts, k_{acc} is a gain, A is the acceleration in meters per square second, β_{acc} is a bias term, and η_{acc} is zero mean white noise. A MEMS rate gyro is based on the transfer of energy between two vibration modes of a structure caused by Coriolis acceleration, thus detecting the rotation. The output of the rate gyro is given by [15]:

$$y_{gyro} = k_{gyro}\Omega + \beta_{gyro} + \eta_{gyro}, \tag{7}$$

where y_{gyro} is in Volts, k_{gyro} is a gain, Ω is the angular rate in radians per second, β_{gyro} is a bias term, and η_{gyro} is zero mean white noise. An aproximate value for the gain should be given on the spec sheet of the sensor. In fact, due to fabrication imperfections, it is not always precisely known. The bias term who is strongly dependent on temperature, should be calibrated prior to each flight.

Quadrotor Control. Control theory is a branch of engineering and mathematics that deals with the behavior of dynamic systems. It utilizes controllers to manipulate the inputs of a system to achieve the desired effect on the output of the system. Perhaps the most common and well-known controller used in control theory is the PID Controller. The general form for a PID controller is described by:

$$u(t) = K_p\big[y_{sp}(t) - y_p(t)\big] + K_i \int_0^t \big[y_{sp}(\tau) - y_p(\tau)\big]d\tau + K_d \left(\frac{dy_{sp}(t)}{dt} - \frac{dy_p(t)}{dt}\right) \quad (8)$$

where u is the control input, y_{sp} the setpoint, y_p is the process variable, and K_P, K_I and K_D are the parameters who regulate the behavior of the PID controller. The main advantages of a PID controller its simple structure and easy implementation of controller [11].
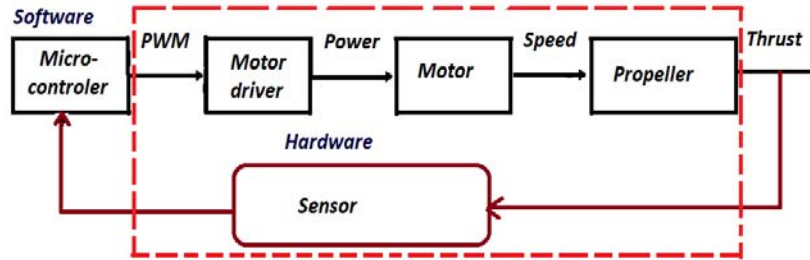

Fig. 3. Quadcopter control

The quadcopter maneuvering stages are obtained by changing the applied thrust force with regard to the exerted weight force of the quadcopter. The quadcopter is controlled by changing the torques of the each motor independently, thus changing the vector of the applied force, schematically shown in figure 3 [20].

3. Results and discussion

Certain aerodynamic parameters must be measured and calculated by experiment bench instead of direct measurements. The thrust coefficient, drag moment coefficient and rotor dynamic parameters are teh most representative of them.

Thrust Testing. Using a Tinius Olsen's Testing Machines (Model H10kS, Hounsfield) different types of commercially available propellers were tested for maximum thrust production versus power input. A software package (QMat Professional software, version 3.0) was used with a PC interfaced with the testing machines. Important information concerning maximum thrust points can be determined from force–distance curves. For all tests, the plunger diameter was 30 mm and with a load cell of 50N (accuracy +/- 0.5% of applied load).

The four motors which we have used in this work are the CL-0820-15 motors from Chaoli Motor. Each motor weighs approximately 4.9 grams and has a

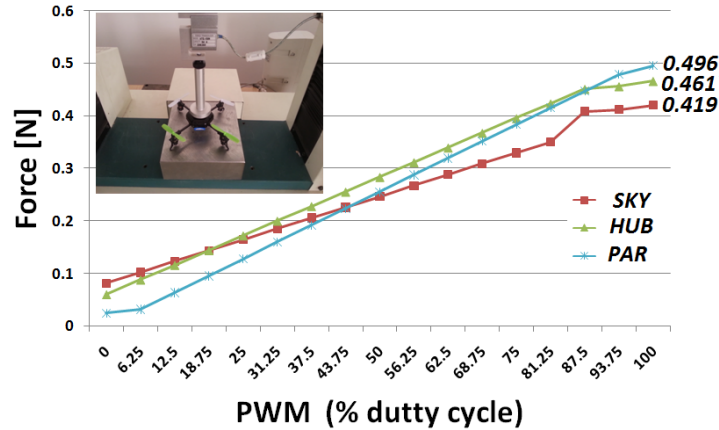max current draw of 4.4 A. It is powered by a Lithium-polymer battery (500mAh - 3.7 V).

Fig. 4. Thrust force vs. PWM inputs

Three different propeller designs were tested with various airfoils, diameters and weight as it is also used in many hobby-range RC quadrotor such as Parrot, Hubsan, and Sky Raynbow.The test was conducted by placing the central hub of quadcopter under the plunger and, as the thrust increased, it pressed load cell to demonstrate the upward force. To increase the thrust, a signal generator provides the PWM signals to the speed controllers. This information was plotted in figure 4 to obtain the regression line which relates thrust to PWM (pulse width modulation). The thrust testing demonstrated that the PAR blade outperformed the others in terms of total thrust produced. The design of the PAR proved to have a better aerodynamic airfoil design compared to the two bladed rotors that we also tested.

Table 1

Propeller characteristics and determinate dynamic parameters

Propeller	Weight[g]	Diam.[mm]	Width[mm]	Pitch [mm]	Thrust[N]	K_T[N/rpm2]	K_T[Nm/rpm2]
PAR	0.37	66	8	7.5	0.496	1.834E-10	1.10E-11
HUB	0.29	55	8	7.25	0.461	1.705E-10	1.02E-11
SKY	0.32	56	8.2	7.25	0.419	1.55E-10	9.30E-12

Assuming the blades are rotating at maximum efficiency speed given on the spec sheet of the motor, the thrust and the drag moment coefficients of the tested rotors are determined from the relations (1-2) and, for reference, are displayed in Table 1.

IMU Sensors Testing. A GY86 board type is used as an IMU, which consists of high quality MEMS sensors. The board containing an MPU 6050 devices which combine a 3-axis gyroscope (sensitivity 131 LSB/deg/s) and a 3-axis accelerometer (sensitivity 16384 LSB/g) on the same silicon die together

with an on-board Digital Motion Processor, a three axes magnetometer (HMC5883L), and embedded pressure sensor (MS5611). All these sensors are connected to an ATMEGA 328P microcontroller which handles all the readings from all sensors through an auxiliary master I^2C bus.

Gyroscopes sense orientation through angular velocity changes and therefore find orientation, but they have a tendency to drift over time because they only sense changes and have no fixed frame of reference [18,19,21]. Accelerometers sense changes in direction with respect to gravity, which can orient a gyroscope to a more exact angular displacement, but the mechanical vibration tends to distort the signal, and thus, incorrect peakes in resulting outputs that produce a gyroscope drift. One solution of this issue is to implement a simple but powerful algorithm, independently applied to sensors output to create a clear signal. Therefore the Complementary Filter, a single line of algebra in code program, is selected in our work for this purpose. This complementary fusion of sensor data is executed with the following equation, for the roll φ and pitch θ axes [19,20]:

$$filtered_{angle} = \alpha \cdot angle_{gyro} + (1 - \alpha) \cdot angle_{acc} , \qquad (9)$$

where, α is related to the time constant, τ, and the sample rate, Δt.

To see the effect of the drift, primarily IMU signal was recorded when the body is in static state. Data was processed in the Arduino board system and sent to a computer through a serial connection for analysis and results. Gyroscopic drift (at a rate of about 0.1°/s) accumulates around each axis of rotation as figure 5 illustrates. The gyroscope accumulate small errors while the accelerometer remains statically near zero because there are no other gravitational forces.
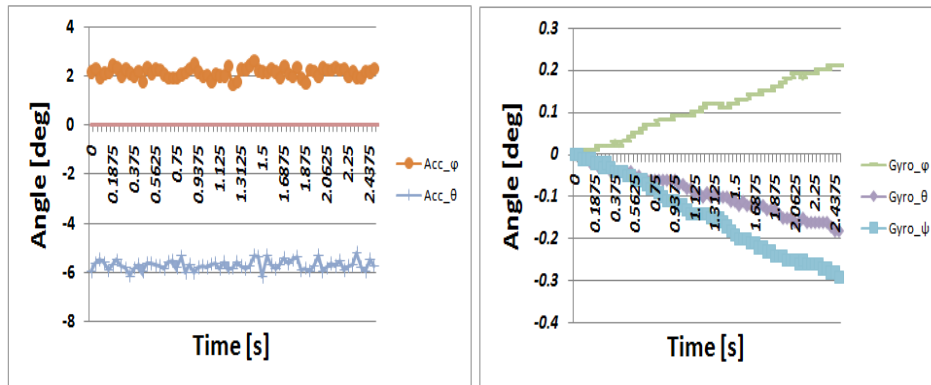

Fig. 5. Static accelerometer and gyroscopic drift

Further, Fig. 6 monitors the outputs of the IMU during the experiments at high motors vibrations. Also, this figure shows how the filter, with the parameters α=0.97 and Δt=0.035s, respond to additional noise due to motor thrusts. Despite vibrations propagating error in the accelerometer short-term output,

complementary filter compensates remarkably well now, and thus, allowed the development of a control algorithm based on sensor outputs.
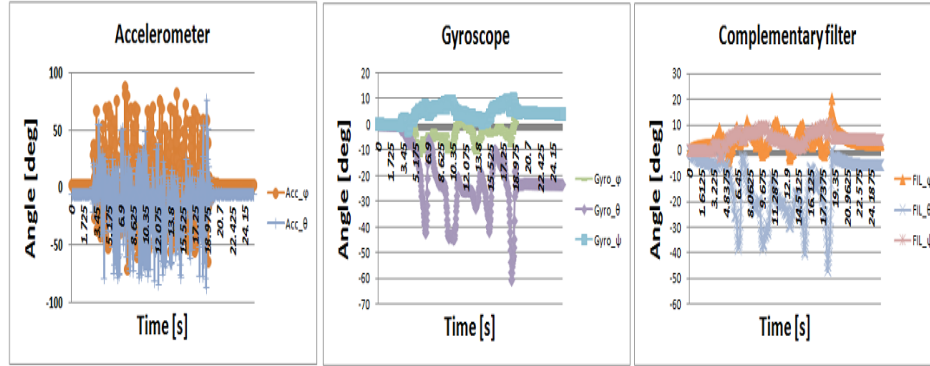

Fig. 6. Testing of IMU sensor: complementary filter

Control design. The main goal is to achieve a stable flight of the quadrocopter, and this is done using a linear PID control strategies. The attitude and altitude stabilization system is composed of *PIDs* that are responsible of keeping the quadcopter in a desired angular state, while keeping its altitude [21]. The PID controller uses a feedback loop to control the rotor angular speed output of the vehicle. Within this loop, the controller uses a combination of the previous output, the current error, and the previous two errors to estimate what adjustments must be made to reach or maintain the desired output. A simulation using Quad-Sim v1.0 MATLAB Tools was conducted to evaluate the theoretical performance of the control theory governing the flight of the quadrotor.
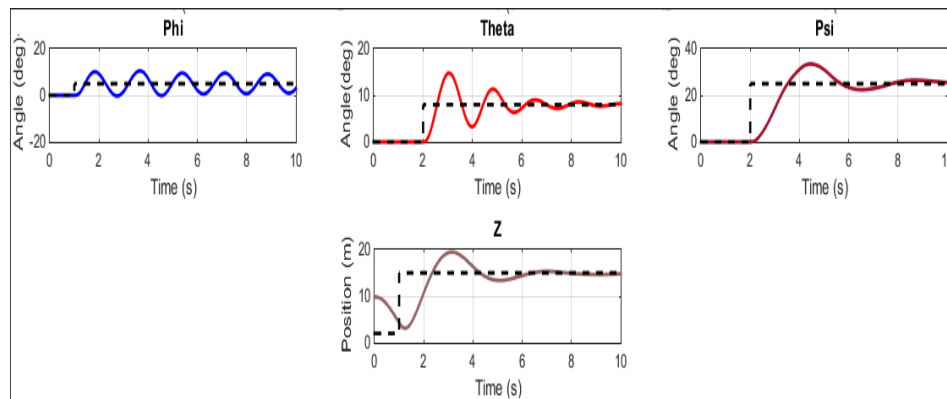

Fig. 7. Attitude and altitude stabilization using PID Controller algorithm

The initial conditions were varied to simulate different maneuvers. The parameter values used for the quadrotor's dynamic model are: M = 0.039 Kg (quadrotor total mass), l = 0.06 m (length of an arm), $Jx=Jy$=6.224e-5 Kg·m^2 and

Jz=1.243e-10 Kg·m^2 (moment of inertia about all three axes), K_T = 1.7e-10 N/rpm^2 and K_τ = 1.02e-11 N·m/rpm^2 (thrust and drag moment coefficients). In simulation presented in figure 7, the task of the controller was to stabilize the orientation φ angle at 5°, θ angle at 8°, ψ angle at 24° and attain a height of 15 meters. Initial condition were: z =10m, $\varphi = \theta = \psi = 0$°, and quadcopter in a stable state. The simulation progresses at 0.035 second intervals, covering a total elapsed time of ten seconds. The altitude controller keeps the distance of the quadcopter to the ground at a desired value. For the first second the quadcopter descended by decreasing all of the rotor velocities from the hover thrust. Then, the descent is stopped by increasing the rotor velocities significantly for the following two seconds. Consequently the quadcopter ascended 20 meters in the first 1.75 seconds. The next second descended five meters, then ascended again. After the ascend the quadcopter remained stable. Simulation results shows that the proposed controller is able to perform the tasks of landing and hovering, and it offers a stable flight. It is also observed that PID controller output has some oscillations and takes more settling time. At low velocities and with small aerodynamic disturbances, proportional integral-derivative (PID) control is fully sufficient for good tracking of commanded attitude [23].

Image Processing. Using the aerial footage taken by drones, farmers can get some useful information about crops, as follows: may reveal patterns of irrigation or soil and fungal infestations that are not visible to the naked eye; the combination of multispectral images, infrared or visible, can create an image of crop that emphasizes healthy plants and those in need; by monitoring the crop at regular intervals, animations can be created, images that show changes over time, revealing problem areas or opportunities to better crop management.
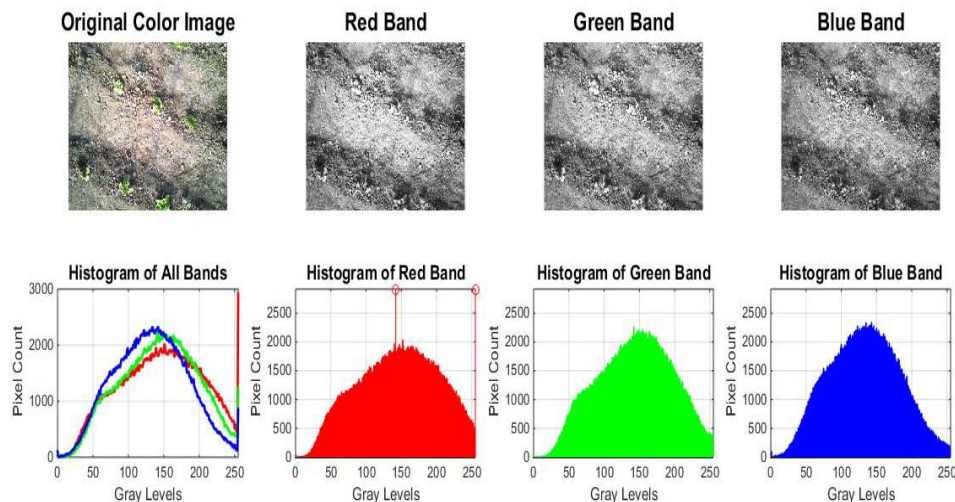

Fig. 8. Aerial view of crop products in greenhouse

After a number of flights, collisions with terrain and imaging, we were able to get valuable information from images collected by the drones on a greenhouse located on the campus of Polytechnic University of Bucharest. Using a low-cost camera available commercially (First Person View 5.8Gz, 0.3 MP) placed under the drone to increase speed and vertically oriented directly towards the ground, we achieved greenhouse indoor ordinary 2D snapshots to assess soil moisture estimation or unhealthy crops. Figure 8 present an example of very simple color detection in RGB color space, extract out the color bands from the original image, and compute the histogram that shows the distribution of intensities in an grayscale image. The close-up inspection method minimizes the effects of soil background noise, hail nets, leaf drooping and shadow with respect to data quality [4]. In order to determine the degree of damage to the structure or to the greenhouse covering material it has been inspected for the exterior, with the camera mounted parallel to the ground. In Figure 9 we can see obviously quite high wear of the polyethylene film. The largest greenhouse film degradation occurs in regions where the film comes into contact with the metal frame of the greenhouse items (marked with X) with high temperature variations.

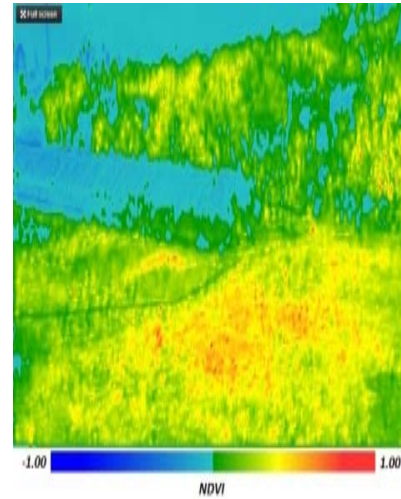Fig. 9. Aerial greenhouse inspection   Fig. 10. NDVI Map

The other factors that influence the mechanical and optical properties of the polyethylene film covering the greenhouse, such as the internal humidity and temperature, biological activity or use of agrochemicals led to the advanced wear. The normalized difference vegetation index (NDVI) is an estimate of the photosynthetically absorbed radiation over the land surfaces. In figure 10, the NDVI is calculated by subtracting the red reflectance values from the near-infrared and divides it by the sum of near-infrared and red bands. Values around zero represent bare soil and values over 0.6 represent dense green vegetation.

6. Conclusions

To some extent, the main goal in the development of precision farming is to replace the traditional agricultural practices. This paper introduced the basic general principles used in designing a quadcopter UAV, which has a wide applicability in modern agriculture. Quadcopter-collected color images are excellent for providing a gross picture of general field health and problems. The use of drones for surveillance of greenhouses can increase crop yields by minimizing the cost of traveling on very large areas and remediation of the issues identified. Also, the drones coupled with smart sensors can be developed to be an effective tool for the future.

Acknowledgements

R E F E R E N C E S

[1] *A. Lebedev,* Design and Implementation of a 6DOF Control System for an Autonomous Quadrocopter, MS Thesis, Julius Maximilian University of Würzburg, 2013.

[2] *P. N. Patel, M. A. Patel, R. M. Faldu, Y. R. Dave* , Quadcopter for Agricultural Surveillance, Advance in Electronic and Electric Engineering, vol. 3, no. 4, 2013, pp. 427-432.

[3] *R. Goel, S. M. Shah, N. K. Gupta and N. Ananthkrishnan*, Modeling, simulation and flight testing of an autonomous quadrotor, Proc. Int. Conf. Environmental and Agriculture Engineering, Bangalore, 2009.

[4] *J. Verbeke, D. Hulens, H. Ramon, T. Goedemé and J. De Schutter,* The Design and Construction of a High Endurance Hexacopter suited for Narrow Corridors, ICUAS'14-The 2014 International Conference on Unmanned Aircraft Systems, May 27-30, 2014, Orlando, Florida, USA.

[5] *R. Austin*, Unmanned Air Systems: UAV Design, Development and Deployment, Wiley, U.K., 2010.

[6] *S. Bouabdallah*, Design and control of quadrotors with application to autonomous flying, PhD Thesis, Julius École Polytechnique Fédérale de Lausanne, 2007.

[7] *M. Becker, R.C.B. Sampaio, S. Bouabdallah, V. Perrot, R. Siegwart,* In-Flight Collision Avoidance Controller Based Only on OS4 Embedded Sensors, J. of the Braz. Soc. of Mech. Sci. & Eng., vol. XXXIV, no. 3 July-September 2012, pp 294-307.

[8] *R. Sugiura, T. Fukagawa, N. Noguchi, K. Ishii, Y. Shibata, K. Toriyama*, Field information system using an agricultural helicopter towards precision farming, Proc. of the 2003 IEEE/ASME International Conference on Advanced Intelligent Mechatronics, vol. 2, July 2003, pp. 1073–1078.

[9] *F. Archer, A. Shutko, T. Coleman, A. Haldin, E. Novichikhin, I. Sidorov,* Introduction, overview, and status of the microwave autonomous copter system MACS, Proc. of the 2004 IEEE International Geoscience and Remote Sensing Symposium, vol. 5, Sep 2004, pp. 3574–3576.

[10] *A. Khan, D. Schaefer, L. Tao, D.J. Miller, K. Sun, M.A. Zondlo, W.A. Harrison, B. Roscoe, D. J. Lary*, Low Power Greenhouse Gas Sensors for Unmanned Aerial Vehicles, Remote Sens., vol. 4, 2012, pp. 1355-1368.

[11] *T. Luukkonnen*, Modelling and control of quadrocopter, Independent Research project in applied mathematics, Aalto University, Espoo, Finland 2011.

[12] *S.K. Phang, K. Li, K.H. Yu, B.M. Chen, T.H. Lee*, Systematic Design and Implementation of a Micro Unmanned Quadrotor System, Unmanned Systems, vol. 2, no. 2, 2014, pp. 1–21.

[13] *M.C. Achtelik, J. Stumpf, D. Gurdan, K.M. Doth*, Design of a Flexible High Performance Quadcopter Platform Breaking the MAV Endurance Record with Laser Power Beaming, Proceedings of the International Conference on Intelligent Robots and Systems, September 2011, San Francisco, pp. 5166-5172.

[14] *S.A. Raza, W. Gueaieb*, Intelligent Flight Control of an Autonomous Quadrotor, Motion Control, Federico Casolo (Ed.), InTech, 2010. Available Online: http://www.intechopen.com/books/motion-control/intelligent-flight-control-of-an-autonomous-quadrotor

[15] *R. W. Beard*, Quadrotor dynamics and control, Lecture notes, Brigham Young University, Provo, USA, 2008.

[16] *A. Gibiansky*, Quadcopter Dynamics, Simulation, and Control, 2012. Available Online: http://andrew.gibiansky.com/downloads/pdf/Quadcopter%20Dynamics,%20Simulation,%20and%20Control.pdf.

[17] *J. Peraire, S. Widnall*, Lecture L29 - 3D Rigid Body Dynamics, MIT OpenCourseWare, Dynamics Fall 2009. Available online: http://ocw.mit.edu.

[18] *M. Elsamanty, A. Khalifa, M. Fanni, A. Ramadan, A. Abo-Ismail*, Methodology for Identifying Quadrotor Parameters Attitude Estimation and Control, International Conference on Advanced Intelligent Mechatronics (AIM) Wollongong, Australia, July 9-12, 2013, pp. 1343-1348.

[19] *B. McCarron*, Low-Cost IMU Implementation via Sensor Fusion Algorithms in the Arduino Environment, FY Thesis, California Polytechnic State University, 2013.

[20] *H.S. Caldera et al.*, A Self-Balancing Quadcopter Design with Autonomous Control, International SAITM Research Symposium on Engineering Advancements, 2014, pp. 146-150.

[21] *N. Ahmad, R. Ariffin, R. Ghazilla and N. M. Khairi*, Reviews on Various Inertial Measurement Unit (IMU) Sensor Applications, International Journal of Signal Processing Systems, vol. 1, no. 2, 2013, pp 256-262.

[22] *R.F. Oliveira, F.T.B. Salvi, E.M. Belo,* Dynamic Modeling, Simulation and Control of an Autonomous Quadcopter Aircraft, Proceedings of COBEM 2009 - 20th International Congress of Mechanical Engineering, November 15-20, 2009, Gramado, Brazil.

[23] *G.M. Hoffmann, H. Huang, S.L. Waslander, C.J. Tomlin*, Quadrotor Helicopter Flight Dynamics and Control: Theory and Experiment, Proceedings of the AIAA Guidance, Navigation, and Control Conference, Hilton Head, South Carolina, 20 - 23 August 2007.